Neurobiology of Disease 52 (2013) 168–176

Contents lists available at SciVerse ScienceDirect

Neurobiology of Disease

journal homepage: www.elsevier.com/locate/ynbdi

Two different interictal spike patterns anticipate ictal activity *in vitro*

Massimo Avoli *, Gabriella Panuccio, Rochelle Herrington, Margherita D'Antuono, Philip de Guzman, Maxime Lévesque

Montreal Neurological Institute and Departments of Neurology & Neurosurgery and of Physiology, McGill University, 3801 Rue University, Montréal, Canada H3A 2B4 PQ

ARTICLE INFO

Article history:
Received 16 October 2012
Revised 26 November 2012
Accepted 14 December 2012
Available online 24 December 2012

Keywords:
4-Aminopyridine
CA3 subfield
Entorhinal cortex
High frequency oscillations
Ictogenesis

ABSTRACT

4-Aminopyridine (4AP, 50 μM) induces interictal- and ictal-like discharges in brain slices including parahippocampal areas such as the entorhinal cortex (EC) but the relation between these two types of epileptiform activity remains undifined. Here, by employing field potential recordings in rat EC slices during 4AP application, we found that: (i) interictal events have a wide range of duration (0.4–3.3 s) and interval of occurrence (1.4–84 s); (ii) ictal discharges are either preceded by an isolated "slow" interictal discharge (ISID; duration = 1.5 ± 0.1 s, interval of occurrence = 33.8 ± 1.8 s) or suddenly initiate from a pattern of frequent polispike interictal discharge (FPID; duration = 0.8 ± 0.1 s; interval of occurrence = 2.7 ± 0.2 s); and (iii) ISID-triggered ictal events have longer duration (116 ± 7.3 s) and interval of occurrence (425.8 ± 42.3 s) than those initiating suddenly during FPID (58.3 ± 7.8 s and 202.1 ± 21.8 s, respectively). Glutamatergic receptor antagonists abolished ictal discharges in all experiments, markedly reduced FPIDs but did not influence ISIDs. We also discovered that high-frequency oscillations (HFOs, 80–500 Hz) occur more frequently during ISIDs as compared to FPIDs, and mainly coincide with the onset of ISID-triggered ictal discharges. These findings indicate that interictal events may define ictal onset features resembling those seen *in vivo* in low-voltage fast activity onset seizures. We propose a similar condition to occur *in vivo* in temporal lobe epileptic patients and animal models.

Introduction

Brain slices maintained *in vitro* generate electrographic seizure-like events – which may represent the equivalent of ictal phenomena seen in patients and in animal models *in vivo* – when $GABA_A$ receptor mediated inhibition is not fully blocked or even enhanced (see for review Avoli and de Curtis, 2011). Procedures capable of eliciting these long-lasting (ictal-like) epileptiform discharges include decreased Mg^{2+} (Köhling et al., 2000; Zhang et al., 2012) or increased K^+ (Jensen and Yaari, 1997; Traynelis and Dingledine, 1988) in the superfusing medium, bath application of the K^+ channel blocker 4-aminopyridine (4AP) (Avoli et al., 1993, 1996; Benini et al., 2003; Dzhala and Staley, 2003; Lillis et al., 2012) or combinations of them (Ziburkus et al., 2006).

Studies performed in adult rodent parahippocampal structures have shown that during 4AP application ictal-like (hereafter refered as ictal) discharges recorded from the entorhinal cortex (EC), amygdala or insular cortex are shortly preceded (and thus heralded) by an isolated "slow" interictal-like spike (ISIS) similar to those recurring at long intervals between successive ictal discharges (see for review Avoli and de Curtis, 2011). This type of interictal activity is largely contributed by $GABA_A$ receptor signaling, and it is associated with transient increases in $[K^+]_o$ (Avoli et al., 1996; Lopantsev and Avoli, 1998b). However, in some experiments, 4AP induces a different type of epileptiform synchronization in the EC; this pattern is characterized by frequent polispike interictal discharges (FPIDs) that are suddenly interrupted by an ictal event (Lopantsev and Avoli, 1998a).

Although the *in vitro* 4AP model has been widely employed to understand the cellular and pharmacological mechanisms underlying ictogenesis (see for review Avoli and de Curtis, 2011), no detailed information on these different patterns of epileptiform synchronization is available. Therefore, we perfomed here a quantitative analysis of the electrophysiological characteristics of interictal- and ictal-like discharges generated during 4AP application by the EC in brain slices that also included the hippocampus proper. However, since ictogenesis in parahippocampal areas can be controlled by hippocampal output activity (Avoli and de Curtis, 2011; Barbarosie and Avoli, 1997; Benini et al., 2003), the EC was either functionally or surgically disconnected from the hippocampus to allow ictal discharge generation. In addition, we established the occurrence of high frequency oscillations (HFOs, 80–500 Hz) during these different patterns of interictal and ictal epileptiform activity. HFOs occur in limbic structures such as the EC and hippocampus, and are thought to reflect the activity of dysfunctional neural networks (Bragin et al., 2004; see for review Jefferys et al., 2012; Engel and Lopes da Silva, 2012).

* Corresponding author. Fax: +1 514 398 8106.
E-mail address: massimo.avoli@mcgill.ca (M. Avoli).
Available online on ScienceDirect (www.sciencedirect.com).

0969-9961/$ – see front matter © 2012 Elsevier Inc. All rights reserved.
http://dx.doi.org/10.1016/j.nbd.2012.12.004

Methods

Slice preparation and maintainance

Male, Sprague-Dawley rats (150–300 g) were decapitated under isoflurane anesthesia according to procedures established by the Canadian Council on Animal Care. All efforts were made to minimize suffering and the number of animals used. The brain was quickly removed and placed in cold, oxygenated artificial cerebrospinal fluid (ACSF). The brain's dorsal side was cut along a horizontal plane that was tilted by a 10° angle along a posterosuperior-anteroinferior plane passing between the lateral olfactory tract and the base of the brainstem (Avoli et al., 1996). Horizontal slices (450 μm thick) containing the EC and the hippocampus were cut from this brain block using a vibratome. Slices were then transferred into an interface tissue chamber where they layed between ACSF (pH 7.4) and humidified gas (95% O_2, 5% CO_2) at a temperature of 32–34 °C. ACSF composition was (in mM): NaCl 124, KCl 2, KH_2PO_4 1.25, $MgSO_4$ 2, $CaCl_2$ 2, $NaHCO_3$ 26, and D-glucose 10. 4AP (50 μM), 6-cyano-7-nitroquinoxaline-2,3-dione (CNQX, 10 μM), 3,3-(2-carboxypiperazin-4-yl)-propyl-1-phosphonate (CPP, 10 μM), and picrotoxin (50 μM) were bath-applied. Chemicals were acquired from Sigma (St Louis, MO, USA). Surgical separation of the EC from the hippocampus proper was performed in some experiments with a knife mounted on a micromanipulator at the beginning of the experiment to further minimize the influence exerted by CA3-driven activity on EC epileptiform synchronization (Barbarosie and Avoli, 1997; Benini et al., 2003).

Electrophysiological recordings

Field potential recordings were made with ACSF-filled, glass pipettes (resistance = 2–10 MΩ) that were connected to high-impedance amplifiers. The recording electrodes were positioned in the EC deep layers. Field potential signals were fed to a computer interface (Digidata 1322A, Molecular Devices, Palo Alto, CA, USA) and acquired and stored using the pCLAMP 9 software (Molecular Devices). Subsequent analysis of these data was made with the Clampfit 9 software (Molecular Devices).

Detection of high-frequency oscillatory events

A multi-parametric algorithm was employed to identify oscillations in each frequency range, using routines based on standardized functions (Matlab Signal Processing Toolbox). Raw field potential recordings were band-pass filtered in the 80–200 Hz and in the 250–500 Hz frequency range using a Finite Impulse Response (FIR) filter. Zero-phase digital filtering was used to avoid phase distortion. A 10 s artifact-free period (40–50 s before the onset of an ictal event for the analysis of HFOs during ictal activity and a 10 s artifact-free time-period for the analysis of HFOs during interictal activity) was selected as a reference for signal normalization. In this way, field potential recordings were normalized using their own reference period.

To be considered as HFO candidates, oscillatory events in each frequency band had to show at least four consecutive cycles having amplitude of 3 SD above the mean of the reference period. The time lag between two consecutive cycles had to be between 5 and 12.5 ms for ripples (HFOs at 80–200 Hz) and between 2 and 4 ms for fast ripples (HFOs at 250–500 Hz). Ripples were kept for analysis only if they were visible in the 80–200 Hz range, whereas fast ripple were kept only if they were visible in the 250–500 Hz range. Oscillatory events containing overlapping ripples and fast ripples were excluded from the analysis.

Field recordings were analyzed for the occurrence of HFOs during the pre-ictal period (from 40 s to the time of ictal onset) and during the ictal period. To account for differences between the duration of ictal events, the ictal event was normalized from 0 (start of the event) to 100 (end of the event). The pre-ictal and ictal periods were then divided in three equal parts and rates of ripples and fast ripples in each part were compared using non-parametric Wilcoxon signed rank tests followed by Bonferroni–Holm corrections for multiple comparisons. This allowed us to evaluate whether ripples or fast ripples predominated during specific moments of the pre-ictal and ictal periods.

Database and analysis

Throughout this study we arbitrarily termed as 'interictal' and 'ictal' the synchronous epileptiform events with durations shorter or longer than 3 s, respectively (*cf.* Traub et al., 1996). Epileptiform activity was recorded during continuous 4AP application and quantitatively analyzed from 84 brain slices. HFOs analysis was performed in 34 of these experiments. Measurements in the text are expressed as means ± SEM and *n* indicates the number of slices included in any specific measurement. Data were compared with non-parametric Mann-Whitney tests and Kruskal–Wallis tests followed by Bonferroni post-hoc tests for multiple comparisons. Wilcoxon signed rank tests were applied to compare rates of HFOs between ictal discharges that were ISIS-triggered or occurred suddenly during FPID. The level of significance was set to $p<0.05$.

Results

Epileptiform activity induced by 4AP in the EC

We recorded both ictal (dotted lines in Figs. 1A and B) and interictal (arrows in Figs. 1A and B) discharges from the EC of "intact" brain slices (n = 84) during 4AP application. Ictal events lasted 100.7 ± 6.1 s (mean ± SEM) and occurred every 316.4 ± 27.1 s while interictal activity had duration of 1.2 ± 0.1 s and interval of occurrence of 21.7 ± 2 s. Simultaneous recordings obtained from EC and CA3 showed that the frequent (0.5–1 Hz) interictal activity generated by CA3 networks (Perreault and Avoli, 1992) did not occur in the EC in these experiments (not illustrated). Hence, we presumed that the EC and the hippocampus were functionally disconnected (*cf.*, Avoli et al., 1996; Benini and Avoli, 2005).

To further ensure that CA3-driven output activity did not influence the epileptiform activity generated by EC neuronal networks, we also performed experiments in slices (n = 19) in which the connections between the hippocampus and this limbic area had been surgically cut. The duration and interval of occurrence of interictal (1.5 ± 0.1 s and 26.2 ± 4.4 s, respectively) and ictal (103.9 ± 11.2 s and 302.9 ± 54.3 s, respectively) discharges recorded in the EC in these surgically cut slices were similar to those seen in the "intact" experiments. Hence, the epileptiform activity induced by 4AP was further analyzed in this study by pooling the data obtained from these two sets of experiments.

As shown in Fig. 1, a striking feature of the interictal activity recorded from the EC was its frequency of occurrence that could be categorized in different experiments as either slowly or frequently occurring (panels A and B, respectively). Interictal events occurring at a slow pace consisted of an initial fast transient followed by a biphasic (Fig. 1Ca) or monophasic (Fig. 1Cb) slow wave of negative polarity, and they will be hereafter termed isolated "slow" interictal spikes (ISISs). In contrast, interictal activity that occurred frequently was usually typified by a negative slow transient associated to multiple population spikes; these interictal events will be hereafter called frequent polispike interictal discharges (FPIDs) (Fig. 1Cc). Interestingly, the mean duration and the mean interval of occurrence of the interictal discharges analyzed in these experiments did not appear to be segregated in two distinct groups but rather they represented a continuum (Figs. 1D and E). However, by plotting the duration *versus* the respective interval of occurrence of interictal activity recorded from the EC in these

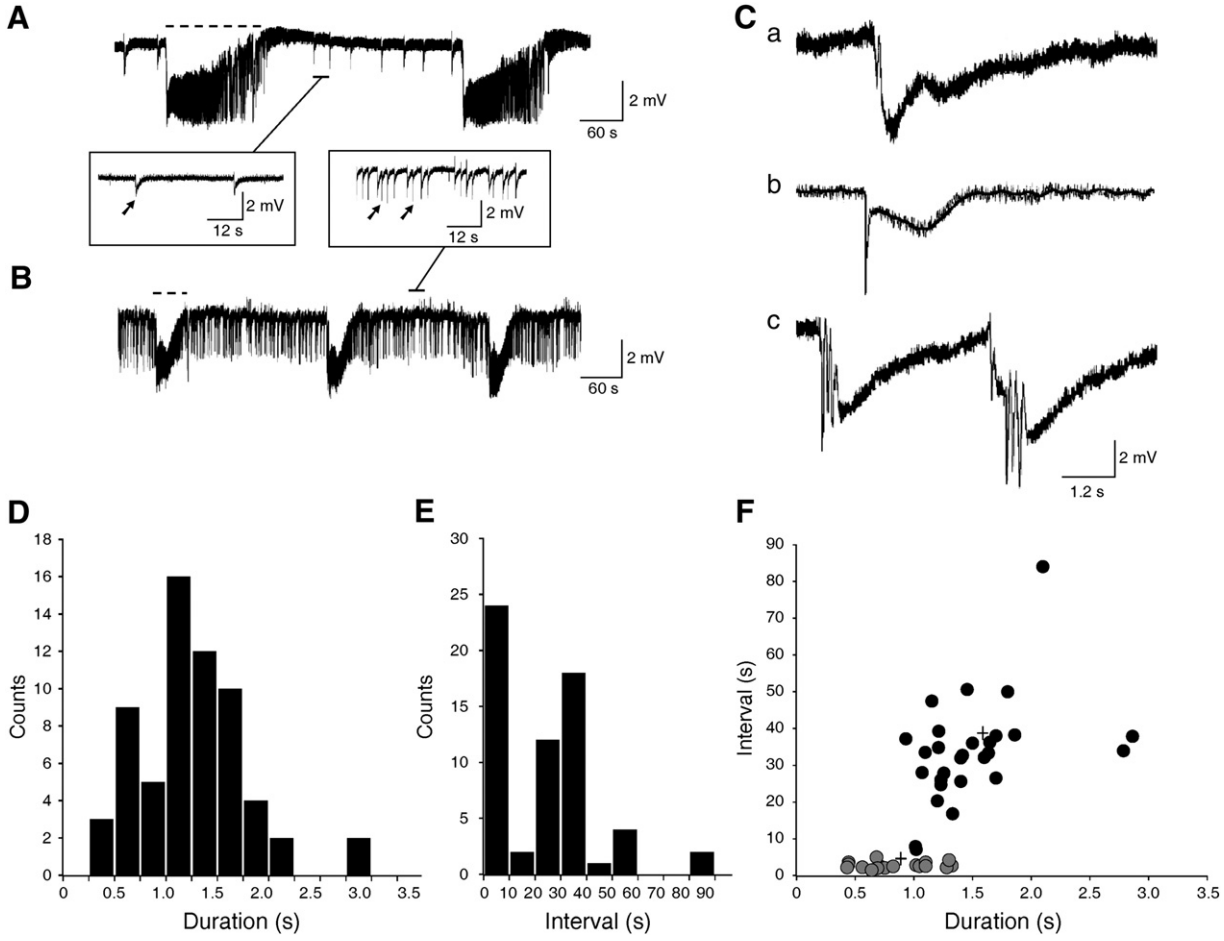

Fig. 1. Synchronous epileptiform activity recorded *in vitro* from the EC. A and B: Interictal (arrows) and ictal (dotted lines) discharges recorded from the EC of two "intact" brain slices during application of 4AP. Note that the rate of the interictal discharges recorded in these two experiments is either slowly (A) or frequently occurring (B). C: Expanded interictal events occurring at a slow pace – also termed ISISs – consist of an initial fast transient followed by a biphasic (a) or monophasic (b) slow wave of negative polarity, while those occurring frequently (c) are characterized by a negative slow transient with multiple population spikes (termed FPIDs). D and E: Histograms of the mean duration and interval of occurrence of the interictal discharges. F: Plot of the duration versus the respective interval of occurrence of interictal activity recorded from these experiments; K-mean cluster analysis identifies two distinct groups (crosses).

slices, we could identify two distinct groups of interictal events that were confirmed by a K-mean cluster analysis (Fig. 1F).

Interictal discharges and ictal discharge onset

Next, we established whether the presence of specific patterns of interictal activity (i.e., ISISs and FPID) correlated with identifiable types of ictal discharge onset as qualitatively suggested by our previous studies (Avoli et al., 1996; Lopantsev and Avoli, 1998a). As illustrated in Fig. 2A, ictal discharges recorded from brain slices that generated ISISs ($n=66$), were characterized in 62 experiments by the occurrence of an ISIS that consistently occurred during the 10 s preceding their onset and could lead to an initial ictal phase that was associated to low-voltage oscillations at 10 Hz. In contrast, ictal activity in slices ($n=18$) that generated FPIDs rose suddenly from an interictal background. The rate of occurrence of interictal spikes that preceded FPIDs did not show any change before ictal onset (Fig. 2B). In the remaining 4 slices generating ISISs during the interictal phase, ictal discharge onset was preceded by an acceleration of the rate of occurrence of interictal events (Fig. 3A).

As illustrated in Fig. 3B, ISIS-triggered ictal discharges had longer duration (116.0 ± 7.3 s; $n=62$) and interval of occurrence (425.8 ± 42.3 s; $n=62$) as compared to those arising suddenly from a FPID background (58.3 ± 7.8 s, $p<0.0001$ and 202.1 ± 21.8 s, $p<0.005$, respectively; $n=18$). As expected, we also found in these experiments that ISISs had duration (1.5 ± 0.1 s) and interval of occurrence (34.5 ± 2.4 s) that were significantly longer than in FPIDs (duration $=0.8\pm0.1$ s, $p<0.0001$; interval of occurrence $=4.5\pm2.4$ s, $p<0.0001$) (Fig. 3C). The duration of the ictal discharges that were characterized in 4 experiments by an accelerating ISIS onset pattern was 75.9 ± 8 s while their interval of occurrence was 319.4 ± 81.9 s. In addition, the interictal activity measured before the appearance of ISIS accelleration lasted 1.3 ± 0.2 s and recurred at an interval of 22.3 ± 4.1 s. However, due to the small number of experiments showing this accelerating ISIS onset pattern we could not perform any statistical comparison with the values obtained from the experiments characterized by ictal discharges that were ISIS-triggered or occurred suddenly.

Syncronous interictal activity recorded during ionotropic glutamatergic receptor antagonism

Previous studies have shown that the typical interictal events recorded in the presence of 4AP (i.e., the ISISs) continue to occur following application of iontropic glutamatergic antagonists while ictal discharges are readily abolished (*cf.*, Avoli and de Curtis, 2011). Hence, we compared the effects induced by concomitant application of CNQX and CPP on the epileptiform activity recorded from slices that generated either ISIDs or FPIDs. As illustrated in Figs. 4A and B, block of glutamatergic transmission abolished ictal discharges in both experimental groups. In contrast, interictal activity was influenced in a

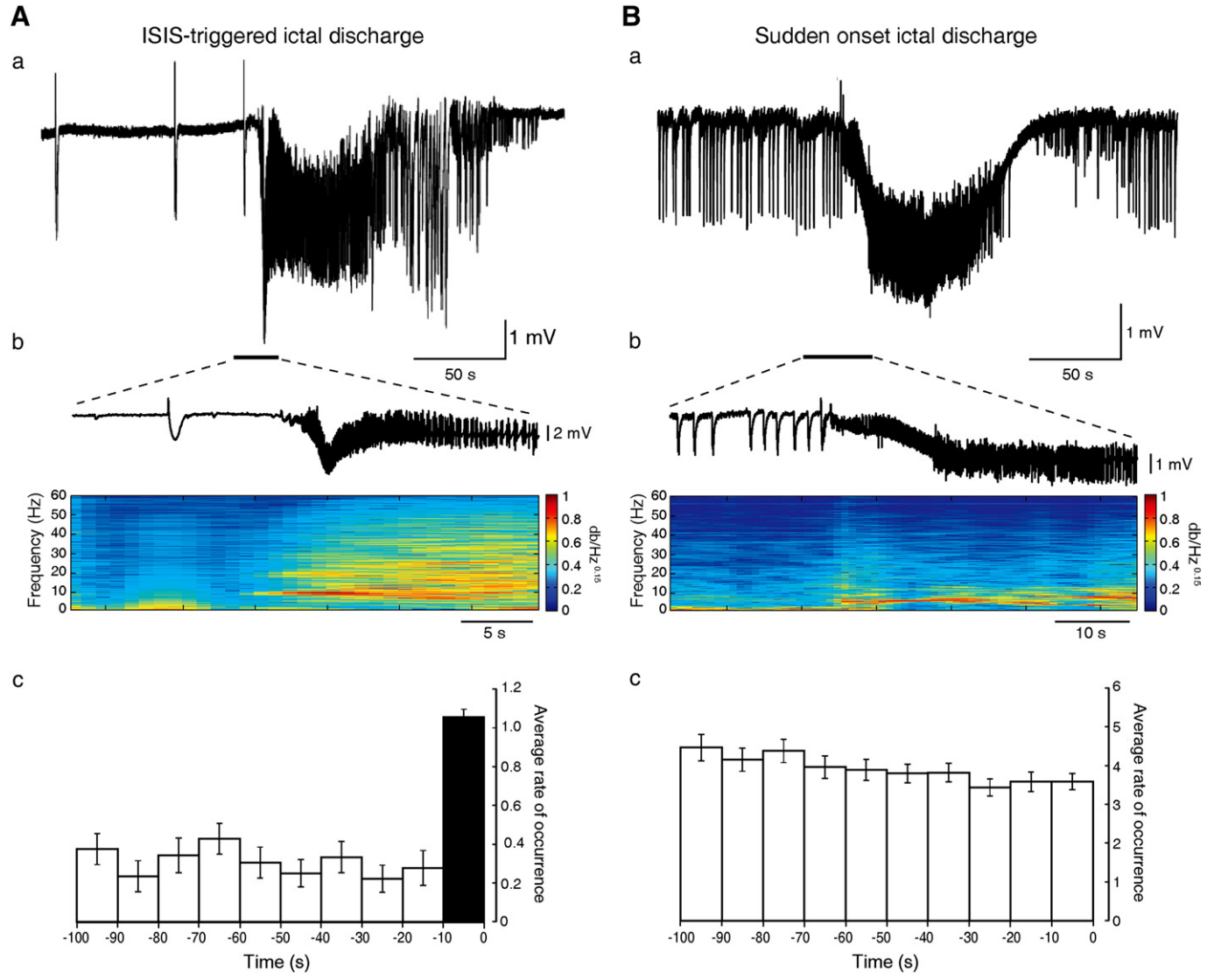

Fig. 2. Interictal activity and ictal discharge initiation. A: Ictal discharge recorded in a brain slice that generated ISISs is shown at two time bases in a and b. In panel b, both the field potential and the power spectrogram corresponding to the onset of the ictal discharge are shown. In this experiment an ISIS occurs approx. 7 s before the ictal onset which is characterized by low-voltage oscillations at 10 Hz. In c, frequency distribution histogram showing the occurrence of ISISs 100 s before the onset of the ictal discharge (n = 22 slices). B: Ictal discharge recorded in a brain slice that generated FPIDs is shown at two time bases in a and b. In panel b both the field potential and the power spectrogram of the onset of the ictal discharge are shown. Note that the ictal discharge onset occurs suddenly from an interictal background that does not show any change in frequency. In c, frequency distribution histogram showing the occurrence of interictal discharges 100 s before the onset of FPIDs (n = 13 slices).

type specific manner by this pharmacological procedure: (i) ISISs continued to occur at similar frequency and with similar duration and amplitude in all experiments (n = 6); while (ii) FPIDs were abolished in 3 of 7 slices and were reduced in duration ($p<0.05$), rate of occurrence ($p<0.001$) and amplitude ($p<0.01$) in the remaining experiments (Figs. 4C–E). As previously reported (*cf.* Avoli and de Curtis, 2011), these synchronous, glutamatergic-independent events were abolished in both types of experiments by applying the $GABA_A$ receptor antagonist picrotoxin thus ruling out that the different effects seen during CNQX + CPP application were not a consequence of ineffective pharmacological blockade of glutamatergic transmission.

High-frequency oscillations in EC during interictal and ictal discharges

Finally, we analyzed the occurrence of HFOs in both ripple (80–200 Hz) and fast ripple (250–500 Hz) frequency ranges during the different types of interictal and ictal activity induced by 4AP in the EC. As illustrated in Figs. 5A and C, HFOs could be observed during both types of interictal activity, and they coincided with the initial component of each discharge. However, the majority of ISISs (69.9%; n = 93 events recorded from 7 slices) and FPIDs (95.7% n = 869 from 7 slices) did not show HFOs. In addition, HFOs occurred more often during ISISs (10.8% for ripples and 18.3% for fast ripples) (Fig. 5B) than during FPIDs (3.6% for ripples and 0.6% for fast ripples) (Fig. 5D).

HFOs also occurred during ictal discharges both when they were characterized by an ISIS-triggered onset (n = 21) and when they emerged suddenly from a FPID background (n = 9) (Fig. 6A). Rates of both ripples ($p<0.005$) and fast ripples ($p<0.001$) were, however, higher during ISIS-triggered as compared to suddenly arising ictal events (Figs. 6A, B). In addition, we found that ISIS-triggered ictal discharges were characterized by a higher proportion of ripples when compared to ictal discharges suddenly arising from a FPID background both during the onset ($p<0.001$) and the middle part ($p<0.05$) of the discharge (Fig. 6C, Ripples). In contrast, there was no significant difference between the two types of ictal discharge, when comparing rates of fast ripples over time (Fig. 6C, Fast Ripples). Ripples and fast ripples

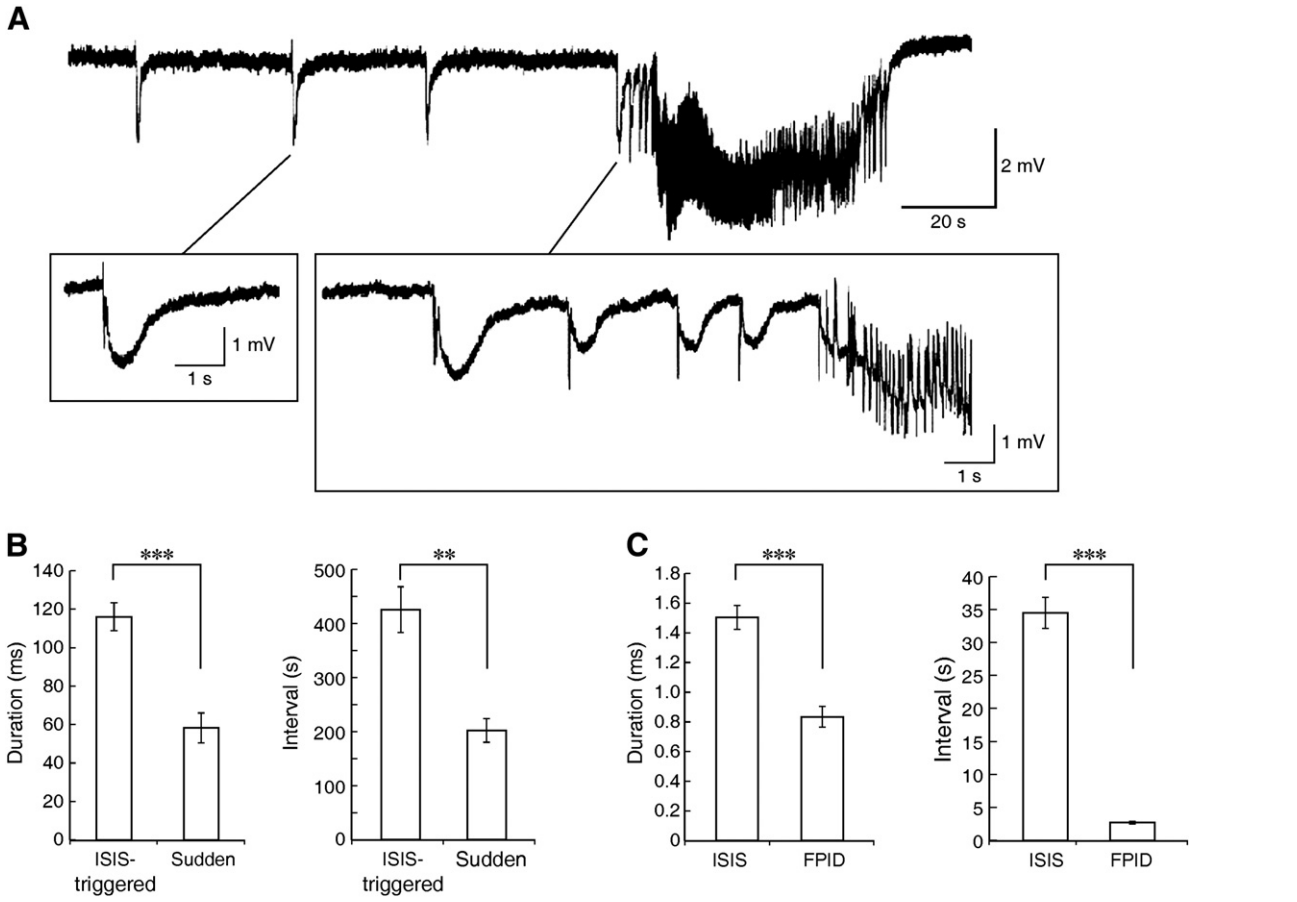

Fig. 3. Interictal activity and ictal discharge initiation. A: Recording of one of the 4 slices generating ISISs that accelerate before ictal discharge onset. In b and c are the events indicated in panel a, shown at faster time scale. B: Plots of the duration and interval of occurrence of ISIS-triggered and sudden onset ictal discharges; note that the former type has longer duration and interval of occurrence. C: Plots of the duration and interval of occurrence of ISIS and FPIDs. Note that both duration and the interval of occurrence of ISISs are higher than those of FPIDs.

did also occur when ictal discharges were heralded by an accellerating ISIS onset pattern. However, due to the small number of experiments we could not statistically compare them with those seen when ictal discharges were ISIS-triggered or occurred suddenly.

Discussion

To the best of our knowledge, this is the first study to address quantitatively the characteristics of the epileptiform activity generated *in vitro* by the rat EC during application of 4AP; the EC plays a prominent role in the generation of seizures induced *in vivo* by electrical stimulation (Stringer and Lothman, 1992) and *in vitro* in several models of ictogenesis (*cf.*, Avoli et al., 2002). In addition, EC dysfunction has been documented in temporal lobe epilepsy patients (Rutecki et al., 1989; Spencer and Spencer, 1994) where its surgical removal may be required for achieving seizure control (Goldring et al., 1992). The main findings of our study can be summarized as follows. First, interictal activity generated by EC neuronal networks presents with a wide range of duration and rate of occurrence that can be epitomized at the two extremes as ISISs and FPIDs. Second, ictal discharges can either be shortly preceded by an ISIS or arise suddenly from a pattern of FPIDs. Third, ISIS-triggered ictal-like events have longer duration and interval of occurrence than those emerging suddenly during FPIDs. Fourth, HFOs are recorded more frequently during ISISs than FPIDs, and their rates are higher during ISIS-triggered as compared to suddenly arising ictal discharges. Finally, we found that EC networks in brain slices that responded to 4AP by generating ISISs continued to do so during application of glutamatergic receptor antagonists; in contrasts, this pharmacological procedure greatly reduced and even abolished FPIDs.

Interictal actvity induced by 4AP in the EC

We have found that the interictal activity recorded in the majority of experiments (i.e., 78.5%) occurred at a slow pace and was characteized by a succession of events predominated by a slow wave. Intracellular recordings obtained from principal neurons in the EC have shown that these interictal spikes – which were termed here as ISISs – correspond to a long-lasting depolarization that triggers few action potentials and is abolished by pharmacological procedures that interfer with $GABA_A$ receptor signaling (Lopantsev and Avoli, 1998b). Moreover, similar slow interictal events have been reported to occur during 4AP treatment in several hippocampal areas (Perreault and Avoli, 1992) and in other cortical (see for review Avoli et al., 2002; Avoli and de Curtis, 2011) and subcortical structures (Lévesque et al., in press). In the remaining experiments (22.5%), we could identify interictal discharges that occurred more frequently and were associated to multiple population spikes, thereby being defined as FPIDs; we have reported that the intracellular events associated to FPIDs consist of robust discharges of action potentials riding over a depolarization (Lopantsev and Avoli, 1998a).

It is well established that 4AP blocks type A outward potassium currents and slows action potential repolarization (Storm, 1987). This action should change neuronal firing but even more so enhance transmitter release at both glutamatergic and GABAergic terminals (see for review Avoli et al., 2002). It is, however, unkown why 4AP can induce

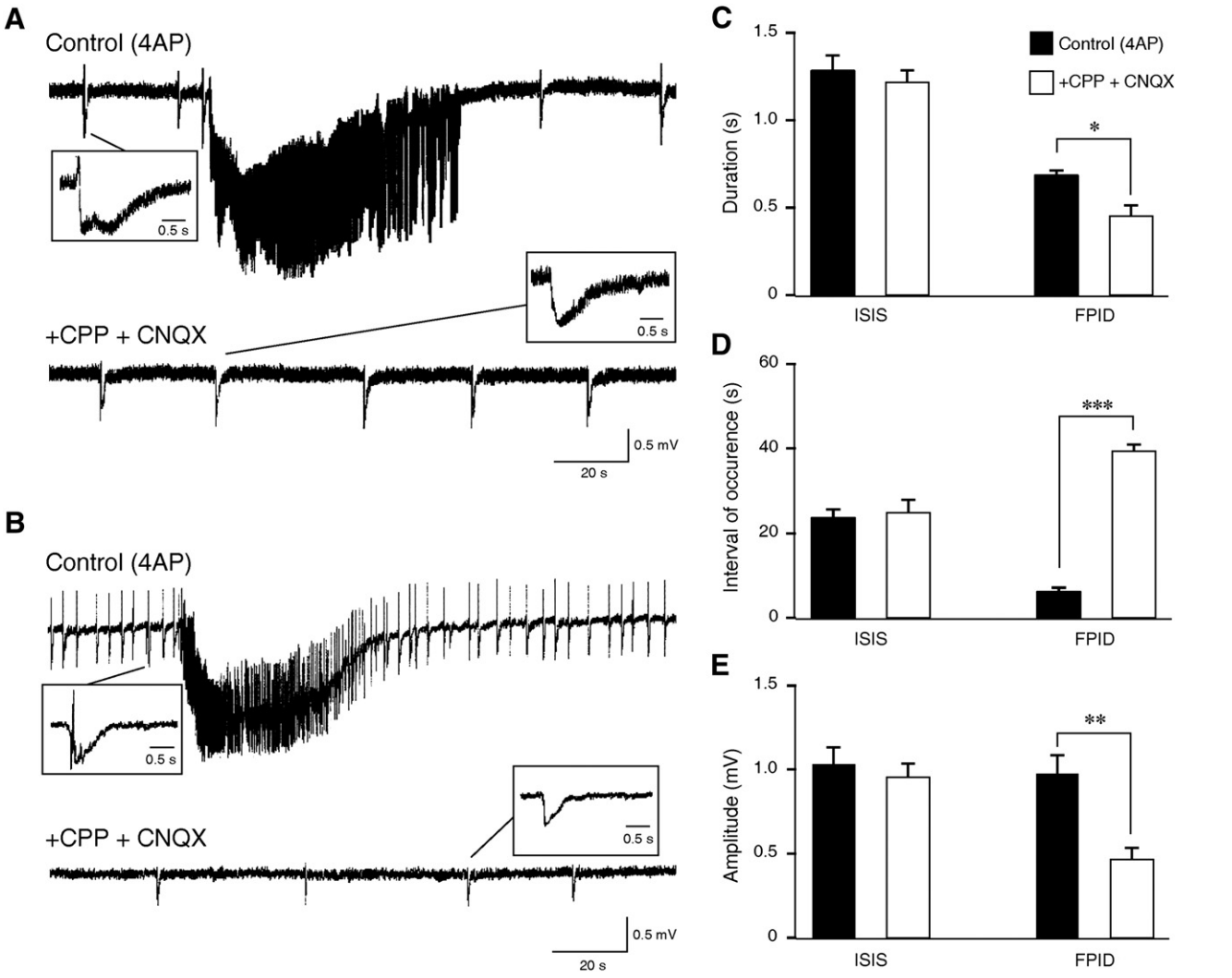

Fig. 4. Effects induced by blockade of glutamatergic transmission in brain slices generating ISIS-triggered and suddenly occurring ictal discharges. A: Concomitant application of CNQX and CPP abolishes ISIS-triggered ictal discharges while ISISs continue to occur with characteristics similar to those seen under control (4AP) conditions. B: The same pharmacological procedure blocks ictal discharges that occur suddenly during FPIDs but also reduce the frequency and the amplitude of the latter events. C–E: Quantification of the effects induced by CNQX + CPP on the two types of interictal discharge. Note that the duration and the amplitude of the events recorded from slices generating ISISs under control conditions are longer and higher than those observed in slices in which the control interictal activity was characterized by FPIDs.

these two types of interictal activity in EC slices that were obtained from animals of similar age and strain. We are inclined to propose that these two patterns mirror a different involvement of GABAergic networks that may result from their different preservation following brain slicing. This view is supported by experiments in which we tested the effects of glutamatergic receptor antagonists on the epileptiform activity induced by 4AP; this pharmacological procedure greatly reduced the duration, the amplitude and the rate of occurrence of FPIDs suggesting that this type of interictal pattern is largely contributed by ionotropic glutamatergic receptor mechanisms. At variance, ISISs continued to occur with amplitudes and rates that were similar to those seen under control conditions (i.e., 4AP treatment). Slow interictal events with electrograhic features similar to the ISISs are recorded during 4AP treatment in the hippocampus, EC and several other cortical structures as well as that they continue to occur during blockade of glutamatergic transmission (see for review Avoli et al., 2002; Avoli and de Curtis, 2011). In addition, the only study available on 4AP-induced interictal activity with characteristics reminiscent of FPIDs reported that these events were abolished by concomitant application of NMDA and non-NMDA glutamate receptor antagonists (Lopantsev and Avoli, 1998a).

We are inclined to exclude that the two different patterns of interictal activity resulted from the influence exerted by hippocampal output activity, and more specifically by CA3-driven interictal discharges (Barbarosie and Avoli, 1997). In line with this view, both ISISs and FPIDs could be recorded in the presence of 4AP from slices in which the connections between the hippocampus and the EC had been surgically cut.

Ictal discharge onsets

The onset of ictal discharges recorded from slices characterized by ISISs was heralded in the majority of experiments by the occurrence of an ISIS that was followed by field oscillations at 10–20 Hz then leading to overt ictal activity; these characteristics were reminiscent of the low-voltage, fast activity onset reported to occur *in vivo* both in epileptic patients (Ogren et al., 2009; Velasco et al., 2000) and in animal models (Bragin et al., 1999, 2005; Lévesque et al., 2012). These results are also similar to those occurring *in vivo* following systemic administration of 4AP in rodents (Lévesque et al., in press). In these experiments we have observed a high proportion of low-voltage fast-onset seizures while in a few cases the ictal discharge onset was characterized by acceleration of ISISs; this second type of onset was indeed similar to the hypersynchronous onset type reported to occur in epileptic patients (Ogren et al., 2009; Velasco et al., 2000), in animal models of temporal

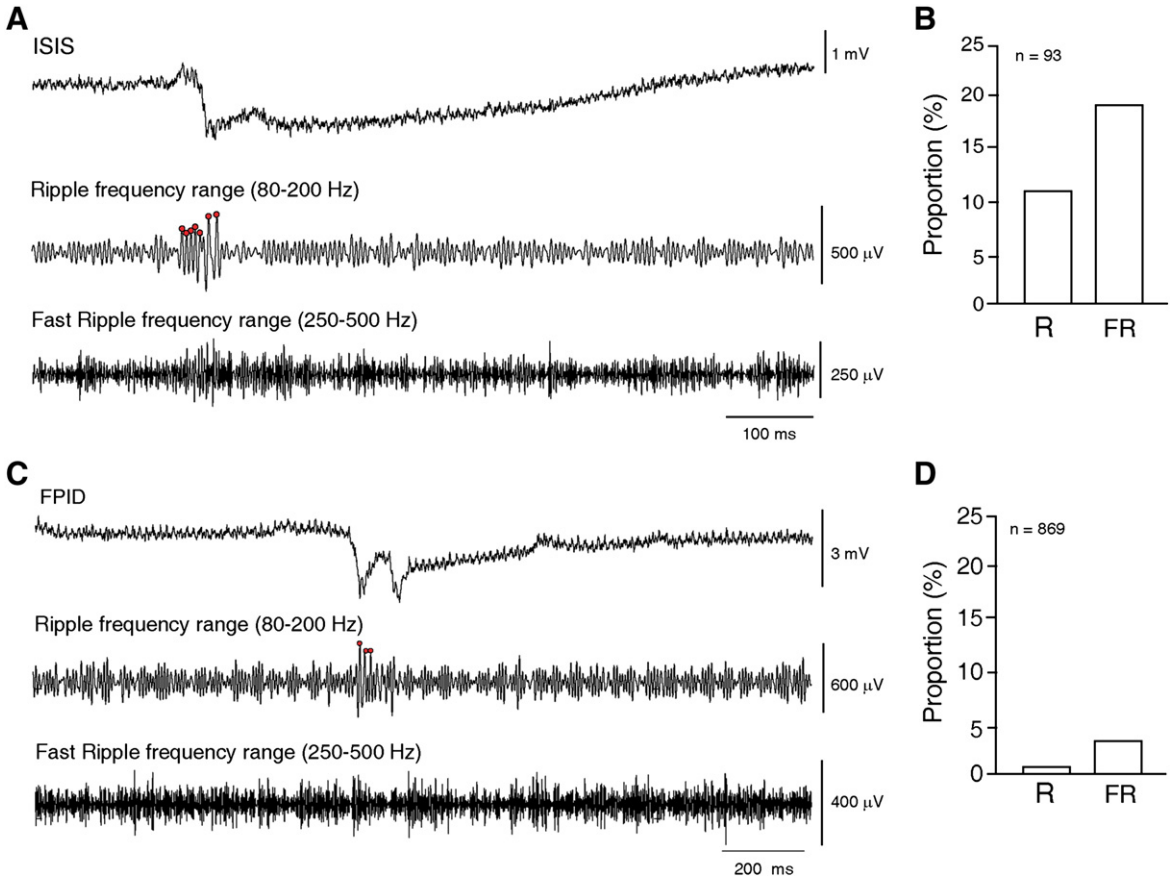

Fig. 5. HFOs and interictal discharges. A: ISIS recorded in EC showing activity in the ripple frequency range (red dots). B. Proportion of slow interictal spikes co-occurring with ripples (R) and fast ripples (FR) showing that ISISs are more often related to ripples and fast ripples compared to FPIDs (*cf.* panel D). C. FPID recorded from EC showing activity in the ripple frequency range (red dots). D: Proportion of FPIDs co-occurring with ripples (R) and fast ripples (FR).

lobe epilepsy (Bragin et al., 1999; Lévesque et al., 2012), and in rodent brain slices superfused with low Mg^{2+} medium (Zhang et al., 2012).

In contrast, ictal discharges recorded in brain slices generating FPIDs occurred suddenly and thus their initiation was not preceded by any detectable change in interictal activity. Remarkably, both the duration and the interval of occurrence of ISIS-triggered ictal events were longer than what was observed in those suddenly rising. These features have also been recently reported in an *in vivo* model of temporal lobe epilepsy where low-voltage fast-onset seizures occurring spontaneously in pilocarpine-treated epileptic rats have longer duration compared to hypersynchronous onset seizures (Lévesque et al., 2012).

Differences in the duration of ISIS-triggered and suddenly arising ictal discharges may be related to, at least, two mechanisms. The first may result from activity-dependent modulation of epileptiform synchronization, i.e., from the higher frequency of occurrence of interictal events in brain slices generating suddenly arising ictal discharges. We have in fact reported that simulating interictal activity by repetitive stimuli delivered at different fixed frequencies influences the duration of 4AP-induced ictal discharges in the EC and specifically that their duration decreases when stimulation is more frequent (D'Arcangelo et al., 2005). The second mechanism, as already discussed above, may relate to a different participation of GABAergic conductances to the two patterns of ictal activity. By using sharp intracellular recordings from EC deep layers, we have found that $GABA_A$-receptor mediated conductances play an active role in the maintenance of 4AP-induced ictal discharges that are initiated by ISISs (Lopantsev and Avoli, 1998b). More recently, Lillis et al. (2012) have reported that pre-ictal $GABA_A$ receptor mediated Cl^- influx produces a positive feedback loop that contributes to the initiation of seizure-like activity in the 4AP *in vitro* model.

HFOs and epileptiform discharges induced by 4AP

HFOs were more frequently observed during ISISs compared to FPIDs. This finding supports the view that ISISs and FPIDs should mirror different neuronal mechanisms as reported in two early intracellular studies performed in the rat EC during 4AP application; it was shown there that ISISs were essentially asociated to synchronous $GABA_A$ receptor-mediated IPSPs (Lopantsev and Avoli, 1998b) while FPIDs mostly mirror glutamatergic depolarizations (Lopantsev and Avoli, 1998a). Accordingly, it has been proposed that ripples reflect IPSPs generated by principal neurons entrained by a network of synchronously active interneurons (Buzsaki et al., 1992; Ylinen et al., 1995) while fast ripples would not strictly depend on GABA receptor signaling (Bragin et al., 2011; Dzhala and Staley, 2003; Engel et al., 2009). Thus, the preferential occurrence of HFOs during ISISs could be caused by the concomitant occurrence of synchronous IPSPs that, interestingly, are also generated in the presence of 4AP even when glutamatergic excitatory transmission is blocked (Avoli and de Curtis, 2011).

HFOs were also observed during ictal discharges, mostly at their onset. However, ISIS-triggered ictal discharges were characterized by a higher rate of ripples compared to ictal discharges suddenly arising from a FPID background, while no difference was seen for fast ripples. This is similar to what has been previously reported in the piriform cortex, since ripples predominated over fast ripples during 4AP-induced ictal discharges, which shared similar morphological features with the ISIS-triggered ictal discharges recorded here from the EC (Panuccio et al., 2012). Our *in vitro* findings are also in agreement with what has been found *in vivo*, since low-voltage fast onset

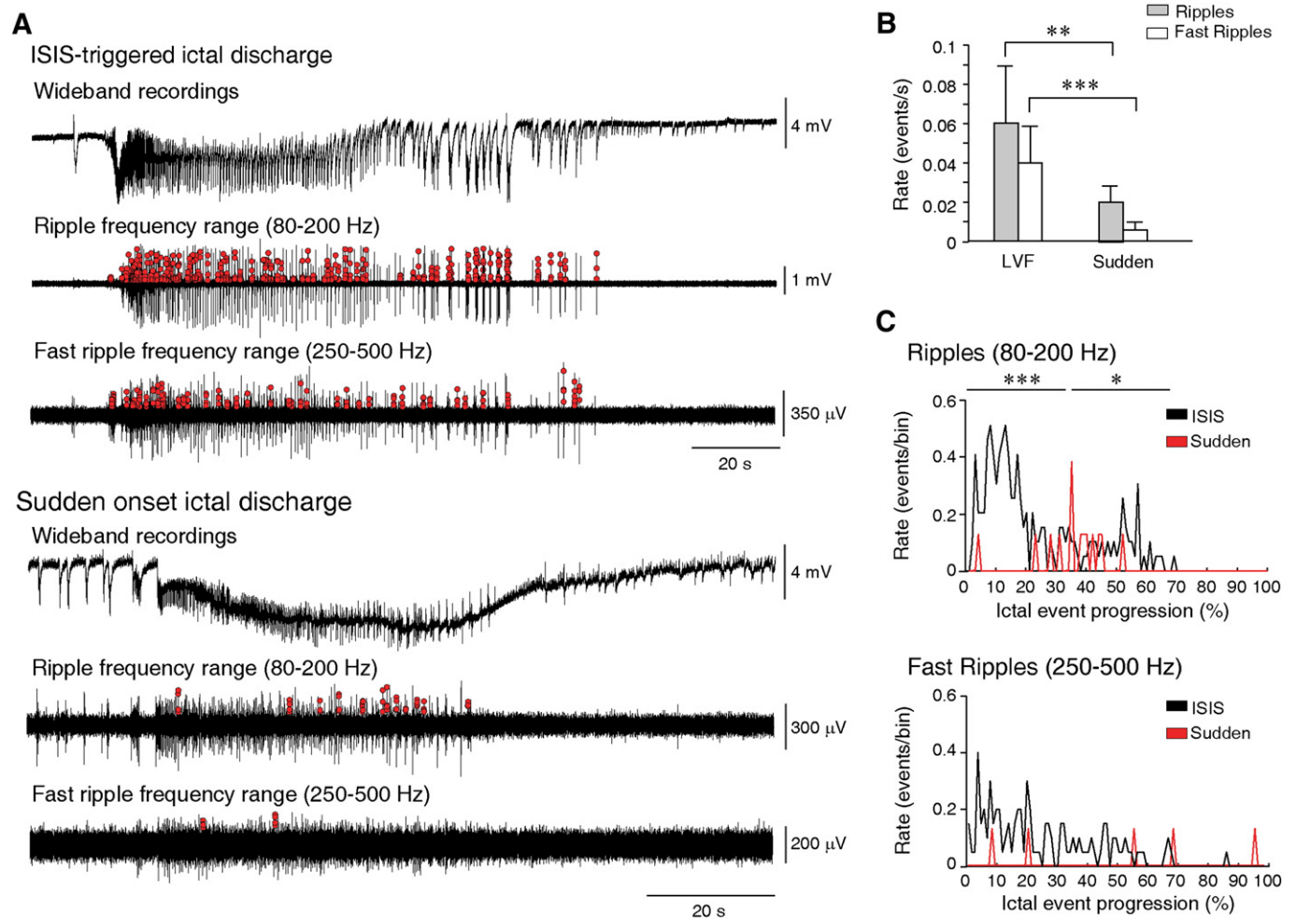

Fig. 6. HFOs and ictal discharges. A: Representative recordings from the EC showing an ISIS-triggerred and a sudden onset ictal discharge with activity in the ripple (80–200 Hz) and fast ripple (250–500 Hz) frequency ranges. HFOs are marked by red dots on each peak of detected oscillations. B: Average rate of occurrence of ripples and fast ripples during each ictal discharge type. ISIS-triggerred ictal discharges contain more HFOs than sudden onset ictal discharges. C: Occurrence of HFOs over time during ictal discharges in the ripple and fast ripple frequency ranges. Ictal discharges were normalized from 0 (start of the ictal discharge) to 100 (end of the ictal discharge) to account for different durations. The first and middle parts of ISIS-triggerred ictal discharges showed significantly more ripples compared to sudden onset ictal discharges. No significant differences were observed for fast ripples. * $p<0.05$, ** $p<0.005$, *** $p<0.001$.

seizures were shown to be related to activity in the ripple frequency range, with a low proportion of fast ripples (Bragin et al., 1999; Lévesque et al., 2012). Thus, the relation between ripples and ISIS-trigerred ictal discharges supports further the hypothetical link between GABAergic synchronization and a specific type of seizure onset. More specifically, ISIS-trigerred ictal discharges, as low-voltage fast-onset seizures observed *in vivo*, could depend on increased interneuron activation, which would therefore explain the high proportion of ripples recorded here compared to fast ripples.

Concluding remarks

Our findings show that interictal spike patterns can define ictal onset features resembling those seen *in vivo* in epileptic patients and in animal models of temporal lobe epilepsy. Specifically, we have found that ISIS occurrence is associated with a type of ictal onset that is remiscent of low-voltage fast onset seizures. Moreover, this interictal pattern, which is associated to synchronous $GABA_A$ receptor-mediated IPSPs, leads to ictal discharges that are more robust than those arising suddenly during FPIDs. We propose that a similar condition may occur *in vivo* both in animal models and in humans.

Ackowledgments

This study was supported by the Canadian Institutes of Health Research (CIHR grants 8109, 74609 and 102710). ML was a recipient of a post-doctoral fellowship from the Savoy Foundation. GP was a recipient of a post-doctoral fellowship from the Savoy Foundation and Epilepsy Canada.

Conflicts of interest

None of the authors has any conflict of interest to disclose.

References

Avoli, M., de Curtis, M., 2011. GABAergic synchronization in the limbic system and its role in the generation of epileptiform activity. Prog. Neurobiol. 95, 104–132.
Avoli, M., Psarropoulou, C., Tancredi, V., Fueta, Y., 1993. On the synchronous activity induced by 4-aminopyridine in the CA3 subfield of juvenile rat hippocampus. J. Neurophysiol. 70, 1018–1029.
Avoli, M., Barbarosie, M., Lucke, A., Nagao, T., Lopantsev, V., Kohling, R., 1996. Synchronous GABA-mediated potentials and epileptiform discharges in the rat limbic system *in vitro*. J. Neurosci. 16, 3912–3924.
Avoli, M., D'Antuono, M., Louvel, J., Köhling, R., Biagini, G., Pumain, R., D'Arcangelo, G., Tancredi, V., 2002. Network and pharmacological mechanisms leading to epileptiform synchronization in the limbic system in vitro. Prog. Neurobiol. 68, 167–207.

Barbarosie, M., Avoli, M., 1997. CA3-driven hippocampal–entorhinal loop controls rather than sustains in vitro limbic seizures. J. Neurosci. 17, 9308–9314.
Benini, R., Avoli, M., 2005. Rat subicular networks gate hippocampal output activity in an in vitro model of limbic seizures. J. Physiol. 566, 885–900.
Benini, R., D'Antuono, M., Pralong, E., Avoli, M., 2003. Involvement of amygdala networks in epileptiform synchronization in vitro. Neuroscience 120, 75–84.
Bragin, A., Engel Jr., J., Wilson, C.L., Vizentin, E., Mathern, G.W., 1999. Electrophysiologic analysis of a chronic seizure model after unilateral hippocampal KA injection. Epilepsia 40, 1210–1221.
Bragin, A., Wilson, C.L., Almajano, J., Mody, I., Engel Jr., J., 2004. High-frequency oscillations after status epilepticus: epileptogenesis and seizure genesis. Epilepsia 45, 1017–1023.
Bragin, A., Azizyan, A., Almajano, J., Wilson, C.L., Engel Jr., J., 2005. Analysis of chronic seizure onsets after intrahippocampal kainic acid injection in freely moving rats. Epilepsia 46, 1592–1598.
Bragin, A., Benassi, S.K., Kheiri, F., Engel, J., 2011. Further evidence that pathologic high-frequency oscillations are bursts of population spikes derived from recordings of identified cells in dentate gyrus. Epilepsia 52, 45–52.
Buzsaki, G., Horvath, Z., Urioste, R., Hetke, J., Wise, K., 1992. High-frequency network oscillation in the hippocampus. Science 256, 1025–1027.
D'Arcangelo, G., Panuccio, G., Tancredi, V., Avoli, M., 2005. Repetitive low-frequency stimulation reduces epileptiform synchronization in limbic neuronal networks. Neurobiol. Dis. 19, 119–128.
Dzhala, V.I., Staley, K.J., 2003. Transition from interictal to ictal activity in limbic networks *in vitro*. J. Neurosci. 23, 7873-7380.
Engel Jr., J., Lopes da Silva, F., 2012. High-frequency oscillations — Where we are and where we need to go. Prog. Neurobiol. 98, 316–318.
Engel, J., Bragin, A., Staba, R., Mody, I., 2009. High-frequency oscillations: what is normal and what is not? Epilepsia 50, 598–604.
Goldring, S., Edwards, I., Harding, G.W., Bernardo, K.L., 1992. Results of anterior temporal lobectomy that spares the amygdala in patients with complex partial seizures. J. Neurosurg. 77, 185–193.
Jefferys, J.G., de la Prida, L.M., Wendling, F., Bragin, A., Avoli, M., Timofeev, I., Lopes da Silva, F.H., 2012. Mechanisms of physiological and epileptic HFO generation. Prog. Neurobiol. 98, 250–264.
Jensen, M.S., Yaari, Y., 1997. Role of intrinsic burst firing, potassium accumulation, and electrical coupling in the elevated potassium model of hippocampal epilepsy. J. Neurophysiol. 77, 1224–1233.
Köhling, R., Vreugdenhil, M., Bracci, E., Jefferys, J.G., 2000. Ictal epileptiform activity is facilitated by hippocampal $GABA_A$ receptor-mediated oscillations. J. Neurosci. 20, 6820–6829.
Lévesque, M., Salami, P., Gotman, J., Avoli, M., 2012. Two seizure onset types reveal specific patterns of high-frequency oscillations in a model of temporal lobe epilepsy. J. Neurosci. 19, 13264–13272.
Lévesque, M., Salami, P., Behr, C., Avoli, M., in press. Temporal lobe systemic epileptiform activity following systemic administration of 4-aminopyridine in rats. Epilepsia http://dx.doi.org/10.1111/epi.12041.
Lillis, K.P., Kramer, M.A., Mertz, J., Staley, K.J., White, J.A., 2012. Pyramidal cells accumulate chloride at seizure onset. Neurobiol. Dis. 47, 358–366.
Lopantsev, V., Avoli, M., 1998a. Laminar organization of epileptiform discharges in the rat entorhinal cortex in vitro. J. Physiol. 509, 785–796.
Lopantsev, V., Avoli, M., 1998b. Participation of $GABA_A$-mediated inhibition in ictal-like discharges in the rat entorhinal cortex. J. Neurophysiol. 79, 352–360.
Ogren, J.A., Bragin, A., Wilson, C.L., Hoftman, G.D., Lin, J.J., Dutton, R.A., Fields, T.A., Toga, A.W., Thompson, P.M., Engel Jr., J., Staba, R.J., 2009. Three-dimensional hippocampal atrophy maps distinguish two common temporal lobe seizure-onset patterns. Epilepsia 50, 1361–1370.
Panuccio, G., Sanchez, G., Lévesque, M., Salami, P., De Curtis, M., Avoli, M., 2012. On the ictogenic properties of the piriform cortex in vitro. Epilepsia 53, 459–468.
Perreault, P., Avoli, M., 1992. 4-Aminopyridine-induced epileptiform activity and a GABA-mediated long-lasting depolarization in the rat hippocampus. J. Neurosci. 12, 104–115.
Rutecki, P.A., Grossman, R.G., Armstrong, D., Irish-Loewen, S., 1989. Electrophysiological connections between the hippocampus and entorhinal cortex in patients with complex partial seizures. J. Neurosurg. 70, 667–675.
Spencer, S.S., Spencer, D.D., 1994. Entorhinal–hippocampal interactions in medial temporal lobe epilepsy. Epilepsia 35, 721–727.
Storm, J.F., 1987. Action potential repolarization and a fast after-hyperpolarization in rat hippocampal pyramidal cells. J. Physiol. 385, 733–759.
Stringer, J.L., Lothman, E.W., 1992. Reverberatory seizure discharges in hippocampal–parahippocampal circuits. Exp. Neurol. 116, 198–203.
Traub, R.D., Borck, C., Colling, S.B., Jefferys, J.G., 1996. On the structure of ictal events in vitro. Epilepsia 37, 879–891.
Traynelis, S.F., Dingledine, R., 1988. Potassium-induced spontaneous electrographic seizures in the rat hippocampal slice. J. Neurophysiol. 59, 259–276.
Velasco, A.L., Wilson, C.L., Babb, T.L., Engel Jr., J., 2000. Functional and anatomical correlates of two frequently observed temporal lobe seizure-onset patterns. Neural Plast. 7, 49–63.
Ylinen, A., Bragin, A., Nádasdy, Z., Jandó, G., Szabó, I., Sik, A., Buzsáki, G., 1995. Sharp wave-associated high-frequency oscillation (200 Hz) in the intact hippocampus: network and intracellular mechanisms. J. Neurosci. 15, 30–46.
Zhang, Z.J., Koifman, J., Shin, D.S., Ye, H., Florez, C.M., Zhang, L., Valiante, T.A., Carlen, P.L., 2012. Transition to seizure: ictal discharge is preceded by exhausted presynaptic GABA release in the hippocampal CA3 region. J. Neurosci. 32, 2499–2512.
Ziburkus, J., Cressman, J.R., Barreto, E., Schiff, S.J., 2006. Interneuron and pyramidal cell interplay during *in vitro* seizure-like events. J. Neurophysiol. 95, 3948–3954.